



**AUTHOR(S):**

**TITLE:**

**YEAR:**

**Publisher citation:**

**OpenAIR citation:**

**Publisher copyright statement:**

This is the \_\_\_\_\_ version of an article originally published by \_\_\_\_\_  
in \_\_\_\_\_  
(ISSN \_\_\_\_\_; eISSN \_\_\_\_\_).

**OpenAIR takedown statement:**

Section 6 of the "Repository policy for OpenAIR @ RGU" (available from <http://www.rgu.ac.uk/staff-and-current-students/library/library-policies/repository-policies>) provides guidance on the criteria under which RGU will consider withdrawing material from OpenAIR. If you believe that this item is subject to any of these criteria, or for any other reason should not be held on OpenAIR, then please contact [openair-help@rgu.ac.uk](mailto:openair-help@rgu.ac.uk) with the details of the item and the nature of your complaint.

This publication is distributed under a CC \_\_\_\_\_ license.

\_\_\_\_\_

## Sophisticated Construction of Binary PdPb Alloy Nanocubes as Robust Electrocatalysts toward Ethylene Glycol and Glycerol Oxidation

Hui Xu, Pingping Song, Carlos Fernandez, Jin Wang, Mingshan Zhu, Yukihide Shiraishi, and Yukou Du

*ACS Appl. Mater. Interfaces*, **Just Accepted Manuscript** • DOI: 10.1021/acsami.8b00532 • Publication Date (Web): 28 Mar 2018

Downloaded from <http://pubs.acs.org> on April 5, 2018

### Just Accepted

“Just Accepted” manuscripts have been peer-reviewed and accepted for publication. They are posted online prior to technical editing, formatting for publication and author proofing. The American Chemical Society provides “Just Accepted” as a service to the research community to expedite the dissemination of scientific material as soon as possible after acceptance. “Just Accepted” manuscripts appear in full in PDF format accompanied by an HTML abstract. “Just Accepted” manuscripts have been fully peer reviewed, but should not be considered the official version of record. They are citable by the Digital Object Identifier (DOI®). “Just Accepted” is an optional service offered to authors. Therefore, the “Just Accepted” Web site may not include all articles that will be published in the journal. After a manuscript is technically edited and formatted, it will be removed from the “Just Accepted” Web site and published as an ASAP article. Note that technical editing may introduce minor changes to the manuscript text and/or graphics which could affect content, and all legal disclaimers and ethical guidelines that apply to the journal pertain. ACS cannot be held responsible for errors or consequences arising from the use of information contained in these “Just Accepted” manuscripts.



1  
2  
3  
4 **Sophisticated Construction of Binary PdPb Alloy Nanocubes as**  
5  
6 **Robust Electrocatalysts toward Ethylene Glycol and Glycerol**  
7  
8 **Oxidation**  
9

10  
11 Hui Xu<sup>†§</sup>, Pingping Song<sup>†§</sup>, Carlos Fernandez<sup>ξ</sup>, Jin Wang<sup>†</sup>, Mingshan Zhu<sup>\*‡</sup>, Yukihide  
12  
13 Shiraishi<sup>Δ</sup>, and Yukou Du<sup>\*†Δ</sup>  
14  
15

16 <sup>†</sup> *College of Chemistry, Chemical Engineering and Materials Science, Soochow*

17  
18 *University, Suzhou 215123, P.R. China*  
19

20  
21 <sup>‡</sup> *Guangdong Key Laboratory of Environmental Pollution and Health, School of*

22  
23 *Environment, Jinan University, Guangzhou 510632, P.R. China*  
24

25  
26 <sup>ξ</sup> *School of Pharmacy and Life Sciences Robert Gordon University U K*  
27

28  
29 <sup>Δ</sup> *Tokyo University of Science Yamaguchi, Sanyo-Onoda-shi, Yamaguchi 756-0884,*

30  
31  
32 *Japan*  
33

34  
35 **ABSTRACT**  
36

37  
38 The design of nanocatalysts by controlling pore size and particle characteristics is  
39  
40 crucial to enhance the selectivity and activity of the catalysis. Thus, we have  
41  
42 successfully demonstrated the synthesis of binary PdPb alloy nanocubes (PdPb NCs)  
43  
44 by controlling pore size and particle characteristics. In addition, the as-obtained  
45  
46 binary PdPb NCs exhibited superior electrocatalytic activity of 4.06 A mg<sup>-1</sup> and 16.8  
47  
48 mA cm<sup>-2</sup> towards ethylene glycol oxidation reaction (EGOR) and 2.22 A mg<sup>-1</sup> and 9.2  
49  
50 mA cm<sup>-2</sup> towards glycerol oxidation reaction (GOR) when compared to the  
51  
52 commercial Pd/C. These astonishing characteristics are attributed to the attractive  
53  
54  
55  
56  
57  
58  
59  
60

1  
2  
3 nanocube structures as well as the large number of exposed active areas. Furthermore,  
4  
5 the bifunctional effects originated from Pd and Pb interactions help to display high  
6  
7 endurance with less activity decay after 500 cycles, showing a great potential in fuel  
8  
9 cells applications.  
10  
11

12  
13 **KEYWORDS:** Binary PdPb nanocubes; Catalysts; Fuel cells; High performance;  
14  
15 Electrooxidation  
16

## 17 18 **1. INTRODUCTION** 19

20  
21 Currently, fuel cells have attracted lots of interest due to their wide application  
22  
23 prospect in our daily lives.<sup>1-2</sup> Ethylene glycol and glycerol, due to their high boiling  
24  
25 point, low toxicity, and less obvious crossover, have attracted considerable attention  
26  
27 for serving as potentially alternative fuels.<sup>3-6</sup> In the research of highly-active  
28  
29 electrocatalysts towards liquid fuels, noble metal platinum has been regarded as the  
30  
31 significant and commonly used material, due to its high activity.<sup>7-8</sup> Nevertheless, there  
32  
33 are some disadvantages associated with Pt such as: high cost, low durability and scare  
34  
35 natural abundance, which have seriously limited its large-scale production.<sup>9-10</sup> To  
36  
37 break this bottleneck, tremendous efforts have been focused on developing an  
38  
39 appropriate substitute for Pt catalysts.<sup>11-13</sup>  
40  
41  
42  
43  
44  
45

46 Recently, well-defined Pd nanocrystals have been of vital significance for  
47  
48 applications in sensing, hydrogen storage and especially in fuel cells due to its high  
49  
50 activity and great tolerance to some CO-like intermediate species in the alkaline  
51  
52 media.<sup>14-18</sup> Regardless of these favorable terms, there are still some problems related  
53  
54 to the Pd nanocrystals such as particle aggregation and poor durability, all of which  
55  
56  
57  
58  
59  
60

1  
2  
3 greatly impede the commercial development of fuel cells technologies.<sup>19-21</sup> Therefore,  
4  
5 considerable attentions have been focused on designing Pd or Pd-based catalysts with  
6  
7 improved electrocatalytic performances.<sup>22</sup> The most promising strategy is to alloy Pd  
8  
9 with a second transition metal, for which can not only gain a higher utilization of Pd,  
10  
11 but also lift the electrocatalytic performances of Pd to a higher level through the  
12  
13 bifunctional, electronic or surface effects.<sup>23-24</sup> Among them, alloying Pd with Pb has  
14  
15 been demonstrated to show excellent electrocatalytic performances due to the  
16  
17 geometric, and electronic effect, as well as the bifunctional mechanism.<sup>25-26</sup> Besides,  
18  
19 the incorporation of Pb into Pd could also offer high resistance to toxic CO-like  
20  
21 species by weakening the bond energy of Pd-CO or by enhancing the electrooxidation  
22  
23 of CO-like species.<sup>27-28</sup>  
24  
25  
26  
27  
28  
29

30 Along with this strategy, morphology control has also been demonstrated to be  
31  
32 an advanced approach for modifying the catalytic properties of Pd nanocrystals,  
33  
34 therefore, enhancing the electrocatalytic performances. Up-to-date, significant  
35  
36 advances have been achieved in the fabrication of Pd-based nanocrystals with  
37  
38 fascinating morphologies. A lot of Pd-based nanocatalysts with unique shapes have  
39  
40 been engineered such as nanowires,<sup>29-30</sup> nanoflowers,<sup>31-32</sup> and nanoframes<sup>33-35</sup>.  
41  
42 Among others, the binary nanocubes with rough surface in particular, have been  
43  
44 proved to expose more active areas,<sup>36-37</sup> which promote the electron mobility and  
45  
46 efficient mass transfer of liquid fuel.<sup>38</sup> In this regard, if we can integrate the  
47  
48 morphology and composition superiorities to fulfill the design of Pd-based  
49  
50 nanocatalysts over size and morphology, it would greatly boost the commercial  
51  
52  
53  
54  
55  
56  
57  
58  
59  
60

development of fuel cells.<sup>39-40</sup>

Herein, we have developed for the first time an advanced method for the synthesis of binary Pd<sub>2</sub>Pb alloy NCs. The key parameter for synthesizing such fascinating Pd<sub>2</sub>Pb NCs structures is the successful introduction of hexadecyltrimethylammonium bromide (CTAB) in the reaction system. In addition, the Pd<sub>2</sub>Pb NCs structures presented unique characteristics such as: highly-dispersed properties as well as synergistic effect. Furthermore, the resulted Pd<sub>2</sub>Pb NCs exhibited greatly enhanced electrocatalytic activities of 4.06 A mg<sup>-1</sup> and 16.8 mA cm<sup>-2</sup>, 2.22 A mg<sup>-1</sup> and 9.2 mA cm<sup>-2</sup> towards EGOR and GOR when compared to Pd/C. Finally, the 500 cycles CV have also demonstrated its superior durability with negligible decay.

## 2. EXPERIMENTAL SECTION

### 2.1 Materials and reagents

Palladium (II) acetylacetonate (Pd(acac)<sub>2</sub>, reagent grade, 99.0%) and oleylamine (OAm) were all purchased from Sigma-Aldrich. Lead (II) acetate (PbAc<sub>2</sub>, analytical reagent, 99.5%), lead (II) chloride (PbCl<sub>2</sub>, analytical reagent, 99%), CTAB (CH<sub>3</sub>(CH<sub>2</sub>)<sub>15</sub>N(Br)(CH<sub>3</sub>)<sub>3</sub>, analytical reagent, 99.0%), and tetra-n-butylammonium bromide (TBAB, analytical reagent, 99.0%) were purchased from Sinopharm Chemical Reagent Co. Ltd. (Shanghai, China). Cetyltrimethylammonium chloride (CTAC, reagent grade, 97%) was purchased from Alfa Aesar (Shanghai, China).

### 2.2 Preparation of PdPb nanocubes (PdPb NCs)

Experimentally, OAm (5 mL), Pd(acac)<sub>2</sub> (7.6mg), PbAc<sub>2</sub> (2.4 mg), and CTAB (36 mg) were added into a vial. After sonicating for 2 h, the glass vial was then transferred

1  
2  
3 to the oil bath and heated to 160 °C in 30 min and kept reacting at 160 °C for another  
4  
5  
6 5 h. The syntheses of Pd<sub>3</sub>Pb NCs and Pd<sub>4</sub>Pb NCs could also be prepared *via* changing  
7  
8 the amounts of PbAc<sub>2</sub> to 3.2 mg and 4.8 mg, respectively while keeping other reaction  
9  
10 conditions the same.

### 13 **2.3 Characterizations**

15  
16 The morphologies and structures of the PdPb NCs were firstly characterized by a  
17  
18 HITACHIHT7700 transmission electron microscope. The FEITecnai F20 transmission  
19  
20 electron microscope was also employed to record the high-angle annular dark field  
21  
22 scanning transmission electron microscopy (HAADF-STEM), high-resolution TEM  
23  
24 (HR-TEM), and energy-dispersive X-ray spectroscopy (EDS) mapping images. A  
25  
26 Thermo Scientific ESCALAB 250 XI X-ray photoelectron spectrometer using 300 W  
27  
28 Al K $\alpha$  radiation was used to recorded the X-ray photoelectron spectroscopy (XPS).  
29  
30 The powder X-ray diffraction (PXRD) patterns were obtained by using X'Pert-Pro  
31  
32 MPD diffractometer (Netherlands PANalytical) with a Cu K $\alpha$  X-ray source ( $\lambda =$   
33  
34 1.540598 Å).

### 40 **2.3 Electrochemical measurements**

42  
43 A standard three-electrode system was employed to perform all the  
44  
45 electrochemical measurements. The electrochemical active surface area (ECSA) was  
46  
47 related to the surface active sites,<sup>1</sup> Therefore the ECSA can be calculated from the  
48  
49 coulombic charge for the reduction of palladium oxide using the following equation:  
50  
51  $ECSA = Q / 0.405 \times Pd_m$ .<sup>41</sup> EGOR was conducted in 1 M KOH + 1 M EG solution and  
52  
53 GOR in 1 M KOH + 1 M glycerol solution. The durability was evaluated by  
54  
55  
56  
57  
58  
59  
60

1  
2  
3 performing the CV for 500 cycles at the sweep rate of  $50 \text{ mV s}^{-1}$ . For comparison, the  
4 commercial Pd/C was used as the reference catalyst.  
5  
6  
7

### 8 **3. RESULTS AND DISCUSSION**

9

10 A simple wet-chemical method has been employed to create a novel class of PdPb  
11 NCs with tunable compositions. The morphological and structural features of Pd<sub>2</sub>Pb  
12 NCs were firstly investigated employing a TEM. The typical TEM images (Figure 1a)  
13 and HAADF-STEM images (Figure 1b) showed that the as-obtained nanocubes are  
14 uniform with a high yield approaching 100%. Through statistics on the size of 50  
15 particles, it was found that the resulted Pd<sub>2</sub>Pb NCs followed a narrow size distribution  
16 with a mean diameter around 10.2 nm (Figure S1). SEM-EDS has been employed also  
17 to confirm the structural compositions and morphologies.  
18  
19  
20  
21  
22  
23  
24  
25  
26  
27  
28  
29  
30  
31  
32  
33  
34  
35  
36  
37  
38  
39  
40  
41  
42  
43  
44  
45  
46  
47  
48  
49  
50  
51  
52  
53  
54  
55  
56  
57  
58  
59  
60

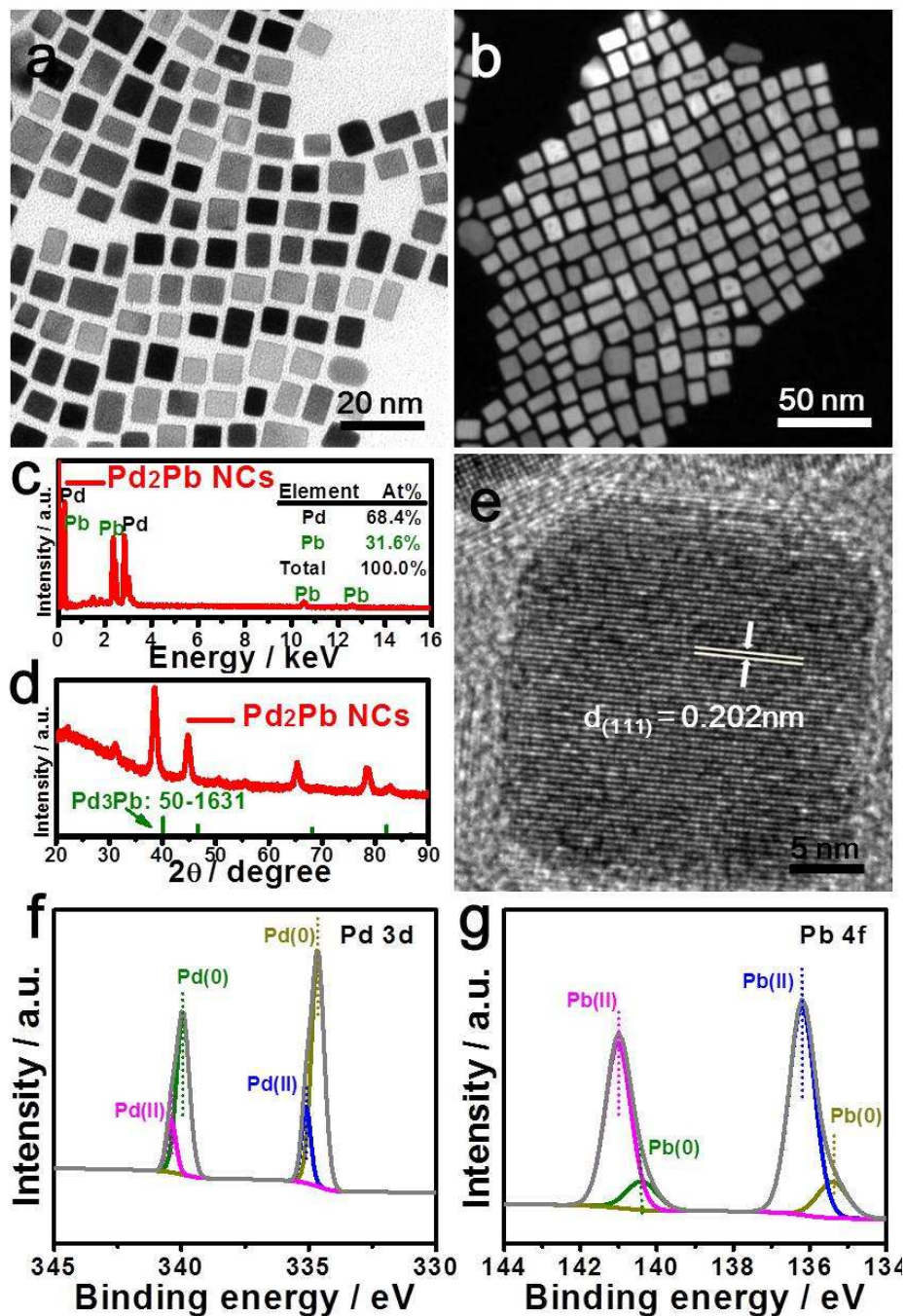


**Figure 1.** (a) TEM, (b) low-magnification HAADF-STEM, (c) SEM-EDS images, (d) PXRD pattern, and (e) HRTEM image. XPS spectra of (f) Pd 3d and (g) Pb 4f in Pd<sub>2</sub>Pb NCs.

Figure 1c illustrates that the atomic ratio of Pd/Pb in Pd<sub>2</sub>Pb NCs is 68.4/31.6,

1  
2  
3 being consistent with the feed ratio. The phase crystals of the samples were  
4 investigated by PXRD (Figure 1d). The PXRD patterns of Pd<sub>2</sub>Pb NCs showed the  
5  
6 approached face-center-cubic (fcc) structure of PdPb alloy, confirming the presence of  
7  
8 PdPb alloy phase in such Pd<sub>2</sub>Pb NCs.<sup>25</sup> In addition, the alloy phase of PdPb was  
9  
10 analyzed by HRTEM (Figure 1e). It was revealed that the adjacent fringe of the NCs  
11  
12 is 0.202 nm, which is associated with the Pd<sub>2</sub>Pb (111) facet, further demonstrating the  
13  
14 alloy phase formation of PdPb.<sup>42</sup> Moreover, the elemental valences and the electronic  
15  
16 coupling effect among Pd and Pb were studied by XPS. As it is displayed in Figure 1f  
17  
18 and g, the binding energy of Pd slightly shift to a higher degree while Pb shift to a  
19  
20 smaller degree when compared with both monometals of Pd and Pb, indicating the  
21  
22 occurrence of charger transfer between Pd and Pb.<sup>43</sup>  
23  
24  
25  
26  
27  
28  
29

30 To further investigate their properties, the Brunauer–Emmett–Teller (BET)  
31  
32 measurements have also been conducted. From the N<sub>2</sub> adsorption–desorption  
33  
34 isotherms in Figure S2, we can find that the as-prepared Pd<sub>2</sub>Pb NCs possessed high  
35  
36 surface area, which is consistent with the analysis of TEM. These results have  
37  
38 revealed that the as-prepared Pd<sub>2</sub>Pb NCs possess a high surface area, thus exposing  
39  
40 more surface active sites available for EG and glycerol.  
41  
42  
43  
44  
45  
46  
47  
48  
49  
50  
51  
52  
53  
54  
55  
56  
57  
58  
59  
60

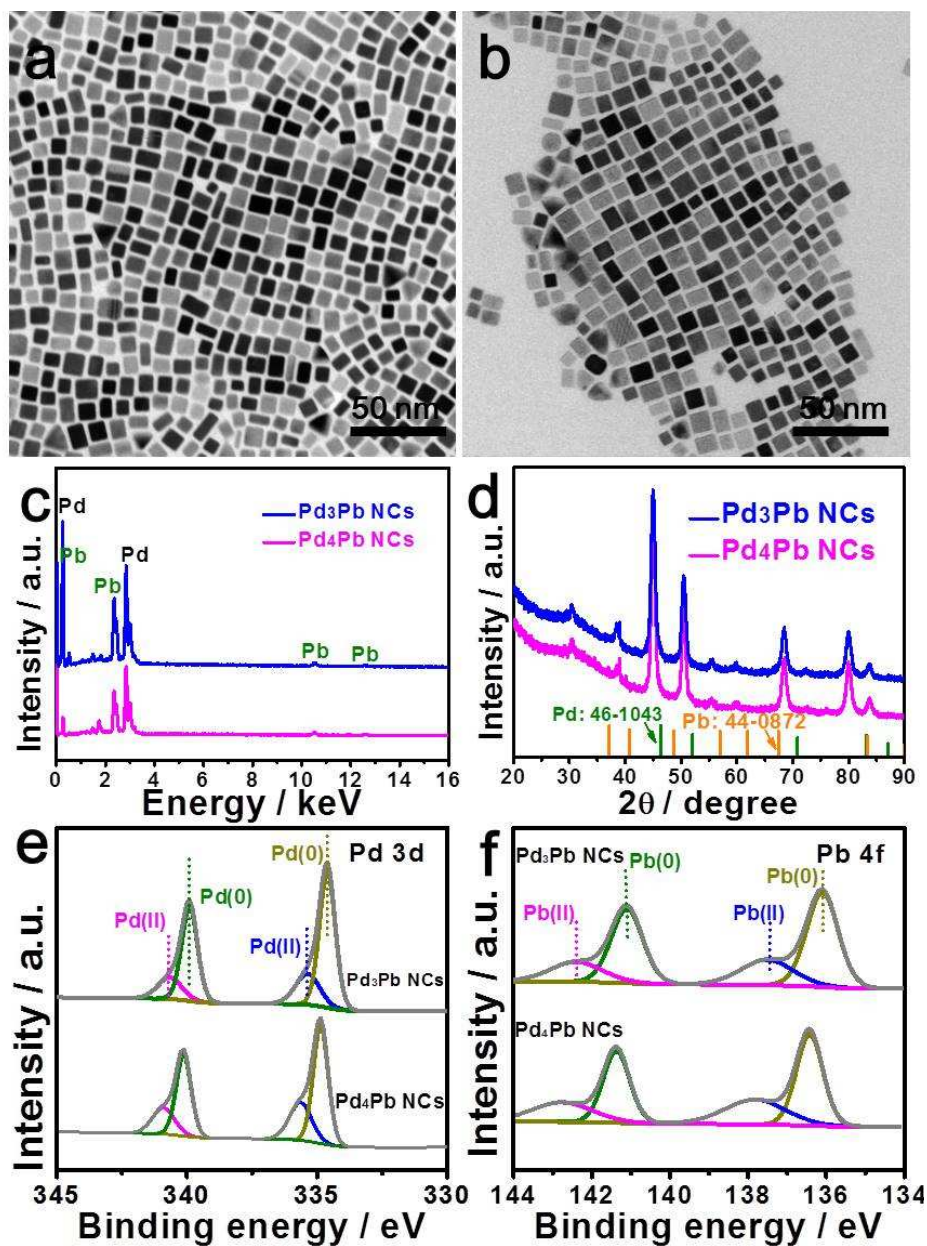


**Figure 2.** TEM images of (a) Pd<sub>3</sub>Pb, (b) Pd<sub>4</sub>Pb NCs, SEM-EDS of (c) Pd<sub>3</sub>Pb and (d) Pd<sub>4</sub>Pb NCs, PXRD patterns of (e) Pd<sub>3</sub>Pb and Pd<sub>4</sub>Pb NCs, (f) XPS spectra of (e) Pd 3d and (f) Pb 4f for Pd<sub>3</sub>Pb and Pd<sub>4</sub>Pb NCs.

It has been demonstrated that the composition can greatly affect the final shape of the nanocrystals. In this regard, we have also taken into consideration the influences of compositions on the morphology, and we have therefore prepared the Pd<sub>3</sub>Pb and

1  
2  
3 Pd<sub>4</sub>Pb NCs *via* the same strategy while adjusting the amount of PbAc<sub>2</sub>. Figure 2a and  
4  
5  
6 b showed that both Pd<sub>3</sub>Pb and Pd<sub>4</sub>Pb nanocrystals also displayed the typical cubic  
7  
8 structure like that of Pd<sub>2</sub>Pb, demonstrating that the large-scale synthesis regardless of  
9  
10 the atomic ratio variation. Through detailed statistics, it was found that the average  
11  
12 diameter of the obtained Pd<sub>3</sub>Pb NCs and Pd<sub>4</sub>Pb NCs were about 12.33 nm and 10.99  
13  
14 nm, respectively. (Figure S3b, d). In addition, the SEM-EDS analyses for Pd<sub>3</sub>Pb and  
15  
16 Pd<sub>4</sub>Pb NCs in Figure 2c and Figure 3 have also revealed that the atomic ratios are also  
17  
18 close to the theoretical values. The PXRD of Pd<sub>3</sub>Pb and Pd<sub>4</sub>Pb NCs were also  
19  
20 analyzed (Figure 2d) to confirm their alloy phase. In addition, both the XRD patterns  
21  
22 of Pd<sub>3</sub>Pb and Pd<sub>4</sub>Pb displayed a slight shift when compared to the standard Pd. The  
23  
24 result indicates the formation of PdPb alloy phases in both Pd<sub>3</sub>Pb and Pd<sub>4</sub>Pb NCs. The  
25  
26 XPS spectra (Figure 2e, f) also illustrated that both metallic states of Pd<sup>0</sup> and Pb<sup>0</sup> play  
27  
28 predominant roles in the composite structures.<sup>28</sup> Pd<sub>1.5</sub>Pb NCs and PdPb NCs have also  
29  
30 been synthesized for comparison purposes. The morphology of the as-prepared  
31  
32 Pd<sub>1.5</sub>Pb NCs and PdPb NCs are characterized by TEM (Figure S4). Pd<sub>1.5</sub>Pb and PdPb  
33  
34 NCs do not have typical cubic structure, which may be ascribed to the addition of  
35  
36 excess amount of lead in the synthesis reaction. Therefore, the amount of lead plays a  
37  
38 significant role in the synthesis of the ideal PdPb NCs.  
39  
40  
41  
42  
43  
44  
45  
46  
47  
48  
49  
50  
51  
52  
53  
54  
55  
56  
57  
58  
59  
60

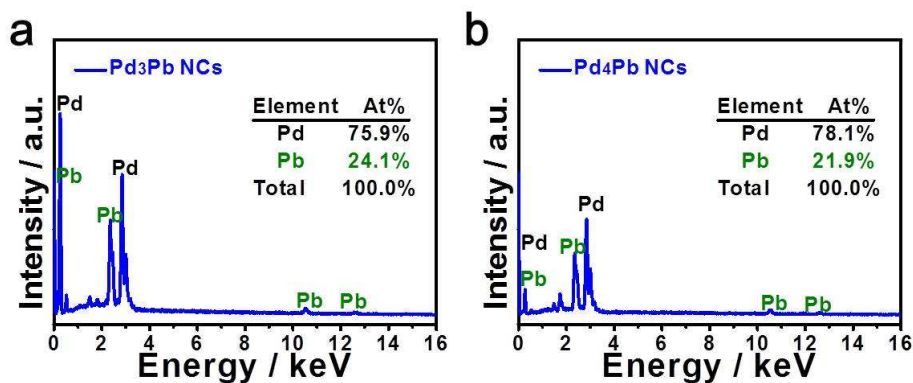
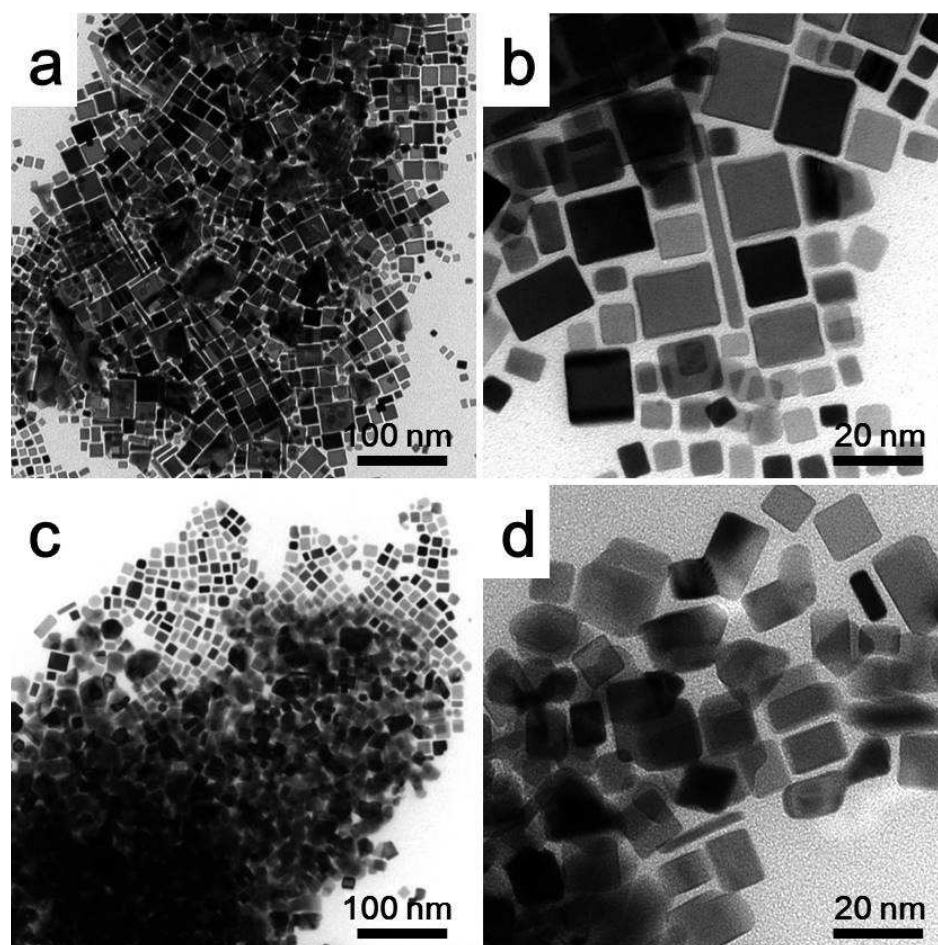


**Figure 3.** The SEM-EDS of (a) Pd<sub>3</sub>Pb NCs and (b) Pd<sub>4</sub>Pb NCs

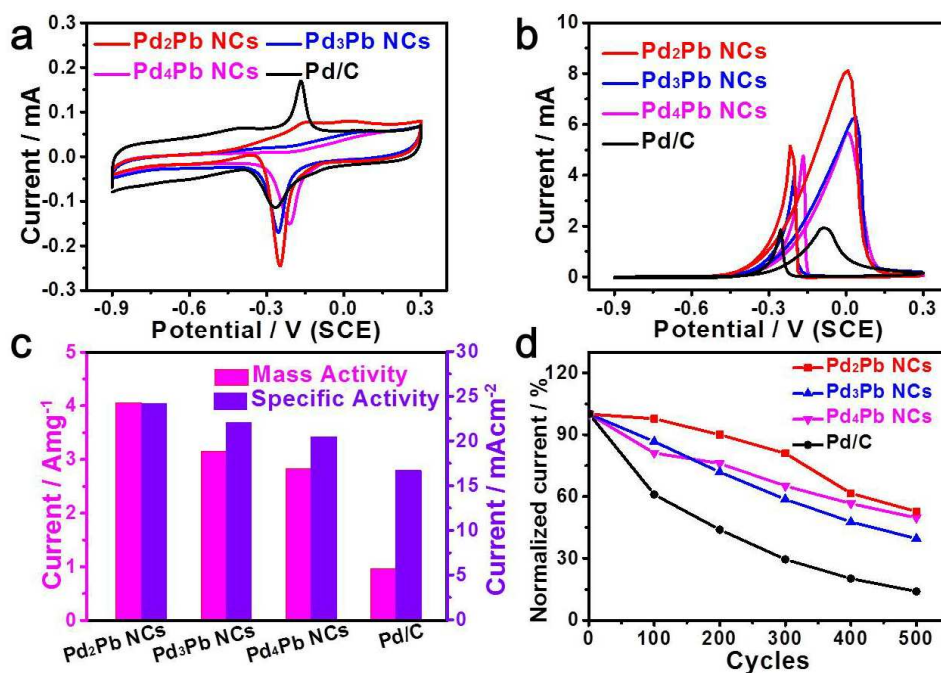
To uncover the formation mechanism, the controlled experiments regarding the reaction parameters have been conducted, and the intermediates from the controlled experiments have also been analyzed by TEM. Among all the experimental parameters, CTAB appears to play a crucial role in controlling the synthesis of PdPb NCs. This can be further demonstrated by the selective adsorption onto specific crystalline surfaces *via* the Van der Waals' forces. In addition, the addition of CTAB significantly decreases the growth rates as well as inducing the anisotropic growth of PdPb NCs with high surface active areas.<sup>44-46</sup> Figure 4a and b showed that the products structures changed dramatically when substituted CTAB with CTAC. When CTAB was changed into TBAB, the morphology of the as-prepared samples changed from NCs to irregular shapes (Figure 4c, d). Therefore, it has been proved that the selective use of CTAB played a significant role in the high-yield production of PdPb NCs. The addition of PbAc<sub>2</sub> was proven to be another significant parameter in the successful preparation of PdPb NCs. As seen in Figure S5, only irregular nanoparticles were obtained when PbAc<sub>2</sub> was replaced with PbCl<sub>2</sub>. These results have revealed that the selective use of CTAB and PbAc<sub>2</sub> was crucial for the successful

1  
2  
3  
4 synthesis of the desirable PdPb NCs.



35 **Figure 4.** TEM images of PdPb nanocrystals prepared in the same condition while  
36 replacing the CTAB with CTAC (a, b) and TBAB (c, d).  
37  
38

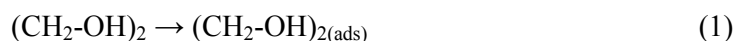
39  
40 Highly uniform PdPb NCs are expected to exhibit outstanding electrocatalytic  
41 performances towards fuel cells. Accordingly, we conducted the EGOR and GOR to  
42  
43 performances towards fuel cells. Accordingly, we conducted the EGOR and GOR to  
44 evaluate their electrocatalytic properties.<sup>47-49</sup> For comparison, the PdPb NCs with  
45 different compositions of Pd<sub>2</sub>Pb NCs, Pd<sub>3</sub>Pb NCs, and Pd<sub>4</sub>Pb NCs were also evaluated.  
46  
47 The commercial Pd/C was also used as benchmark electrocatalysts for further  
48 comparison. The ECSA values of Pd<sub>2</sub>Pb, Pd<sub>3</sub>Pb, Pd<sub>4</sub>Pb and Pd/C were found to be  
49  
50 24.2, 22.1, 20.5, and 16.7 m<sup>2</sup> g<sup>-1</sup>, respectively.  
51  
52  
53  
54  
55  
56  
57  
58  
59  
60



**Figure 5.** CV curves of Pd<sub>2</sub>Pb NCs, Pd<sub>3</sub>Pb NCs, Pd<sub>4</sub>Pb NCs, and Pd/C catalysts in (a) 1 M KOH solution and (b) 1 M KOH + 1 M EG solution. (c) The catalytic activities of these four electrocatalysts. (d) Durability comparisons of these four types of electrocatalysts for 500 cycles.

The EG electrooxidation measurements were conducted in 1 M KOH + 1 M EG solution. Figure 5b displayed the typical CV of these four nanocatalysts. The oxidation peaks for the electrocatalysts were found to be at the potential around -0.05 V. Figure 5c illustrates the mass and specific activities of Pd<sub>2</sub>Pb NCs, Pd<sub>3</sub>Pb NCs, Pd<sub>4</sub>Pb NCs and commercial Pd/C. The Pd<sub>2</sub>Pb NCs exhibited the highest peak current density value of 4.06 A mg<sup>-1</sup> in comparison to all the investigated electrocatalysts. The aforementioned value is therefore, 4.23, 1.43, and 1.29 times greater than that of Pd/C (0.96 A mg<sup>-1</sup>), Pd<sub>4</sub>Pb NCs (2.83 A mg<sup>-1</sup>), and Pd<sub>3</sub>Pb NCs (3.15 A mg<sup>-1</sup>), respectively. Besides, the resulted Pd<sub>2</sub>Pb NCs also displayed superior specific activity

1  
2  
3 of 16.8 mA cm<sup>-2</sup> towards EGOR which was superior than that of Pd/C (5.8 mA cm<sup>-2</sup>),  
4 Pd<sub>4</sub>Pb NCs (13.8 mA cm<sup>-2</sup>), and Pd<sub>3</sub>Pb NCs (14.3 mA cm<sup>-2</sup>). Moreover, the  
5  
6 comparison results from Table S1 further confirmed its superior electrocatalytic  
7  
8 activity towards EGOR. The superior electrocatalytic activity of Pd<sub>2</sub>Pb towards  
9  
10 EGOR can be attributed to the electron and surface effect in the PdPb alloy.<sup>50</sup> Besides,  
11  
12 it has been demonstrated that the electrocatalytic activity of Pd can also be improved  
13  
14 to a higher level after the incorporation of Pb because of the formation of sufficient  
15  
16 oxygen species, which can react with some intermediates and release the surface  
17  
18 active sites of Pd.<sup>49, 51</sup> However, a redundant Pb will block the exposed surface active  
19  
20 sites of Pd, thus lowering the activity of Pd.<sup>43</sup> Therefore, the addition of Pb at a certain  
21  
22 content (Pd : Pb = 2:1) can significantly increase the catalytic activity towards the  
23  
24 EGOR. The successive CVs of 500 cycles have also been operated in 1 M KOH + 1  
25  
26 M EG solution to evaluate EGOR durability (Figure S6). The results showed that the  
27  
28 Pd<sub>2</sub>Pb NCs gave the highest durability. In addition, the mass activity only decayed by  
29  
30 47.3 % which was much superior than those of commercial Pd/C (86.1%), Pd<sub>4</sub>Pb  
31  
32 NCs (60.1%) and Pd<sub>3</sub>Pb NCs (50.1%), respectively (Figure 5d), indicating its better  
33  
34 electrocatalytic durability towards EGOR. The oxidation mechanism of (CH<sub>2</sub>OH)<sub>2</sub> is  
35  
36 shown below, in which the reaction system can be oxidized to nontoxic C<sub>2</sub>O<sub>4</sub><sup>2-</sup>,  
37  
38 showing superior electrocatalytic performances.<sup>52-53</sup>



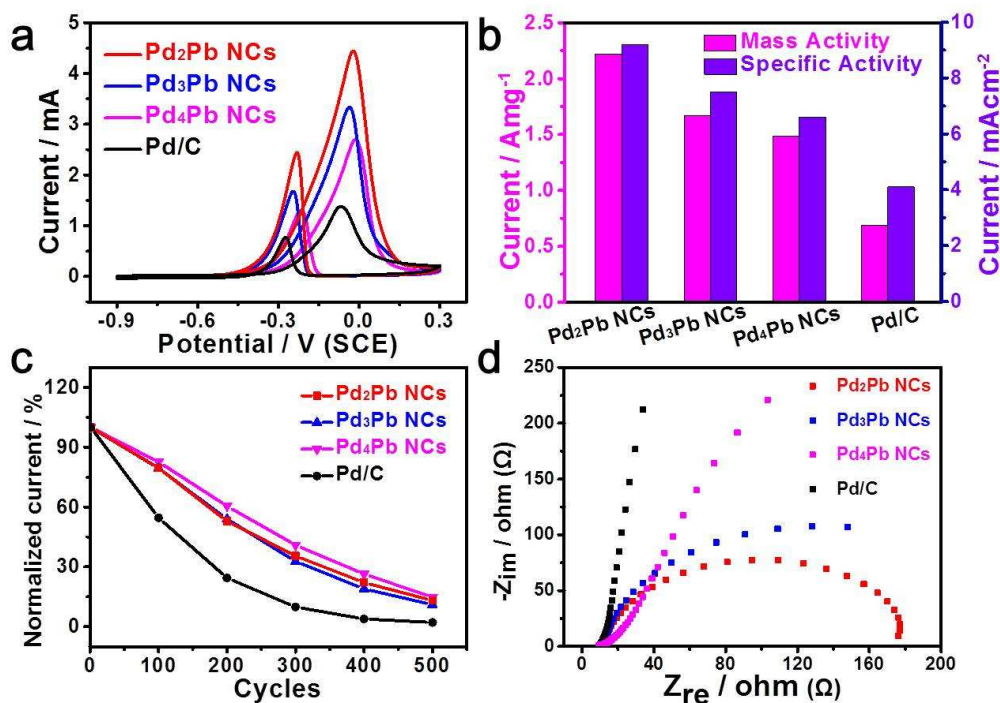


**Figure 6.** CV curves of Pd<sub>2</sub>Pb NCs, Pd<sub>3</sub>Pb NCs, Pd<sub>4</sub>Pb NCs, and commercial Pd/C catalysts in (a) 1 M KOH + 1 M glycerol solution, as well as its (b) corresponding histogram. (c) Durability comparisons of these four types of electrocatalysts for 500 cycles. (d) Nyquist plots of these four electrocatalysts operated in 1 M KOH + 1 M glycerol solution at the potential of -0.1 V.

As for the GOR, the activity variations among these four different catalysts are also similar with that in EGOR (Figure 6a, b). Remarkably, the Pd<sub>2</sub>Pb NCs also showed the highest mass activity of 2.22 A mg<sup>-1</sup> which was much greater than commercial Pd/C (0.69 A mg<sup>-1</sup>), Pd<sub>4</sub>Pb NCs (1.48 A mg<sup>-1</sup>), and Pd<sub>3</sub>Pb NCs (1.67 A mg<sup>-1</sup>). In addition, the Pd<sub>2</sub>Pb NCs also showed the highest specific activity of 9.2 mA cm<sup>-2</sup>, which is 2.24, 1.39, and 1.23 times higher than those of Pd/C (4.1 mA cm<sup>-2</sup>), Pd<sub>4</sub>Pb NCs (6.6 mA cm<sup>-2</sup>) and Pd<sub>3</sub>Pb NCs (7.5 mA cm<sup>-2</sup>), respectively. Moreover, the

durability measurements of these four types of electrocatalysts for the GOR were also conducted *via* repeating the CV scans of 500 cycles. As seen in Figure 4c and Figure S7, after the 500 successive cycles, 14.8% of the initial mass activity was maintained for the nanocubic Pd<sub>2</sub>Pb NCs, which is much better than those of Pd/C (2.1%), Pd<sub>4</sub>Pb NCs (11.0%) and Pd<sub>3</sub>Pb NCs (13.2%). Furthermore, after the 500 successive cycles, the compositions and shapes of PdPb NCs were largely maintained, highlighting the outstanding long-term stability (Figure 7, Figure S8-S10). It has been demonstrated that Pb could lead to the generation of ample oxygenated species and boost the activation of active sites of Pd. All of these fascinating properties have made Pb a perfect catalyst ligand.<sup>54-55</sup> Similar to the EGOR, the main products for GOR were the CO<sub>3</sub><sup>2-</sup>, indicating the complete oxidation of glycerol. The GOR mechanism was shown as follows:<sup>56</sup>

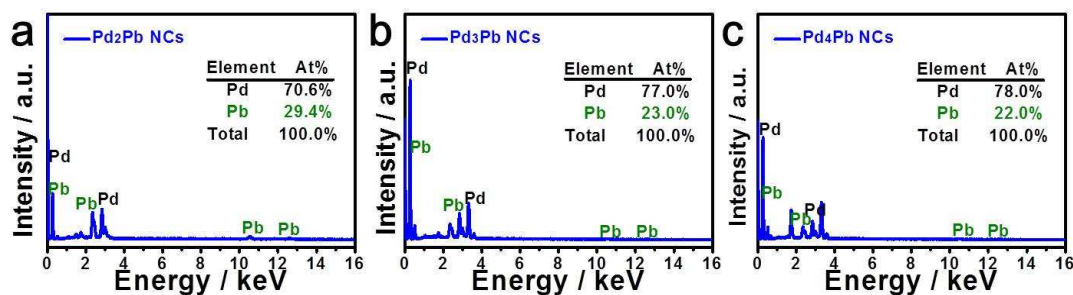
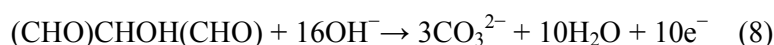
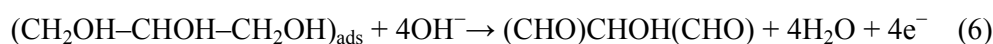
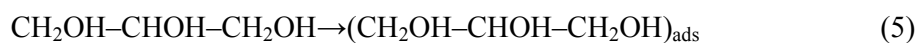


**Figure 7.** The SEM-EDS of (a) the Pd<sub>2</sub>Pb NCs, (b) Pd<sub>3</sub>Pb NCs, and (c) Pd<sub>4</sub>Pb NCs after electrochemical durability test.

1  
2  
3  
4 The electrochemical impedance spectroscopy (EIS) was carried out at the  
5  
6 potential of -0.1 V to study their electrochemical reaction processes, where the  
7  
8 diameter is a crucial parameter for evaluating the electrical conductivity of the  
9  
10 as-prepared electrocatalysts.<sup>57</sup> As seen in Figure 6d, the order of the diameter  
11  
12 impedance arc (DIA) of these electrocatalysts was as follows: Pd/C > Pd<sub>4</sub>Pb NCs >  
13  
14 Pd<sub>3</sub>Pb NCs > Pd<sub>2</sub>Pb NCs. The resulted Pd<sub>2</sub>Pb NCs gave the smallest electron transfer  
15  
16 resistance and the best electrical conductivity, which was consistent with their  
17  
18 outstanding electrocatalytic performances.<sup>58</sup> In this work we clearly demonstrated that  
19  
20 the as-obtained PdPb NCs showed a great enhancement towards electrocatalytic  
21  
22 activity and reusability. The enhanced performance of the uniform PdPb NCs reported  
23  
24 herein is likely to be attributed to the integration of the nanocubic structures and  
25  
26 synergistic effects between the Pd and Pb.  
27  
28  
29  
30  
31

#### 32 33 **4. CONCLUSIONS** 34 35

36 In conclusion, an advanced and yet efficient strategy has been developed for the  
37  
38 design of well-defined cubic PdPb nanocatalysts with a high yield. The controlled  
39  
40 experiments have revealed that the preparation of PdPb NCs were CTAB-dependent.  
41  
42 This new class of PdPb nanocatalysts have the distinctive characteristics of being  
43  
44 ultra-uniform as well as having a nanocubic structure. Those unique characteristics  
45  
46 are responsible for greatly improving the electrocatalytic performances of fuel cells  
47  
48 oxidation reactions. Impressively, the optimized Pd<sub>2</sub>Pb NCs gave the best  
49  
50 electrocatalytic performances towards EGOR and GOR, suggesting a great potential  
51  
52 for fuel cells. The approach based on tuning the morphology of nanocatalysts can also  
53  
54  
55  
56  
57  
58  
59  
60

1  
2  
3 be extended to some other nanomaterials to generate nanocrystals with desirable  
4 nanostructures.  
5  
6

#### 7 8 ASSOCIATED CONTENT 9

10  
11 The Supporting Information is available free of charge on the ACS Publications  
12 website. EDX, XRD, TEM and XPS of the as-prepared samples. CVs, scan cycling  
13 experiments and chronoamperometric curves of Pd<sub>2</sub>Pb NCs, Pd<sub>2</sub>Pb NCs, Pd<sub>2</sub>Pb NCs  
14 and commercial Pd/C modified electrode on electrocatalytic oxidation of ethylene  
15 glycol and glycol.  
16  
17  
18  
19  
20  
21  
22

#### 23 24 AUTHOR INFORMATION 25

##### 26 27 Corresponding Author 28

29  
30 E-mail: mingshanzhu@yahoo.com(M.Z.); duyk@suda.edu.cn (Y.D.). Tel:  
31  
32 +86-512-65880089, Fax: +86-512-65880089;  
33  
34  
35

##### 36 37 Author Contributions 38

39 § These authors contributed equally. The manuscript was written through  
40 contributions of all authors. All authors have given approval to the final version of the  
41 manuscript.  
42  
43  
44

##### 45 46 Notes 47

48  
49 The authors declare no competing financial interest.  
50

#### 51 52 ACKNOWLEDGMENT 53 54 55 56 57 58 59 60

This work was supported by the National Natural Science Foundation of China (Grant No. 51373111, 21603111), the Suzhou Industry (SYG201636), the project of scientific and technologic infrastructure of Suzhou (SZS201708), the Priority Academic Program Development of Jiangsu Higher Education Institutions (PAPD). In addition, CF would like to express his gratitude to RGU for support.

## References

1. Zhu, C.; Guo, S.; Dong, S., PdM (M = Pt, Au) bimetallic alloy nanowires with enhanced electrocatalytic activity for electro-oxidation of small molecules. *Adv. Mater.* **2012**, *24*, 2326-2331.
2. Wang, A. L.; Xu, H.; Feng, J. X.; Ding, L. X.; Tong, Y. X.; Li, G. R., Design of Pd/PANI/Pd sandwich-structured nanotube array catalysts with special shape effects and synergistic effects for ethanol electrooxidation. *J. Am. Chem. Soc.* **2013**, *135*, 10703-10709.
3. Hong, W.; Shang, C.; Wang, J.; Wang, E., Bimetallic PdPt nanowire networks with enhanced electrocatalytic activity for ethylene glycol and glycerol oxidation. *Energy Environ. Sci.* **2015**, *8*, 2910-2915.
4. Xin, L.; Zhang, Z.; Qi, J.; Chadderton, D.; Li, W., Electrocatalytic oxidation of ethylene glycol (EG) on supported Pt and Au catalysts in alkaline media: reaction pathway investigation in three-electrode cell and fuel cell reactors. *Appl. Catal. B Environ.* **2012**, *125*, 85-94.
5. Kannan, R.; Kim, A. R.; Nahm, K. S.; Lee, H. K.; Yoo, D. J., Synchronized synthesis of Pd@C-RGO carbocatalyst for improved anode and cathode performance for direct ethylene glycol fuel cell. *Chem. Commun.* **2014**, *50*, 14623-14626.
6. Kannan, R.; Kim, A. R.; Nahm, K. S.; Yoo, D. J., Manganese-titanium-oxide-hydroxide-supported palladium nanostructures – A facile electrocatalysts for the methanol, ethylene glycol and xylitol electrooxidation. *Int. J. Hydrogen Energy* 2016, *41*, 6787-6797.
7. Bu, L.; Guo, S.; Zhang, X.; Shen, X.; Su, D.; Lu, G.; Zhu, X.; Yao, J.; Guo, J.; Huang, X., Surface engineering of hierarchical platinum-cobalt nanowires for efficient electrocatalysis. *Nature Commun.* **2016**, *7*, 11850.
8. Sun, X.; Li, D.; Ding, Y.; Zhu, W.; Guo, S.; Wang, Z. L.; Sun, S., Core/shell Au/CuPt nanoparticles and their dual electrocatalysis for both reduction and oxidation reactions. *J. Am. Chem. Soc.* **2014**, *136*, 5745-5749.
9. Huang, J.; Zhu, Y.; Liu, C.; Zhao, Y.; Liu, Z.; Hedhili, M. N.; Fratalocchi, A.; Han, Y., Fabricating a homogeneously alloyed AuAg shell on Au nanorods to achieve strong, stable, and tunable surface plasmon resonances. *Small* **2015**, *11*, 5214-5221.
10. Du, W.; Yang, G.; Wong, E.; Deskins, N. A.; Frenkel, A. I.; Su, D.; Teng, X., Platinum-tin oxide core-shell catalysts for efficient electro-oxidation of ethanol. *J. Am. Chem. Soc.* **2014**, *136*, 10862-10865.
11. Yang, C. W.; Chanda, K.; Lin, P. H.; Wang, Y. N.; Liao, C. W.; Huang, M. H., Fabrication of Au-Pd core-shell heterostructures with systematic shape evolution using octahedral nanocrystal cores and their catalytic activity. *J. Am. Chem. Soc.* **2011**, *133*, 19993-20000.

12. Hong, X.; Wang, D.; Cai, S.; Rong, H.; Li, Y., Single-crystalline octahedral Au-Ag nanoframes. *J. Am. Chem. Soc.* **2012**, *134*, 18165-18168.
13. Kannan, R.; Kim, A. R.; Lee, H.-K.; Yoo, D. J., Coordinated fast synthesis of electrocatalytic palladium nanoparticles decorated graphene oxide nanocomposite for fuel cell applications. *J. Nanosci. Nanotechnol.* **2015**, *15*, 5711-5717.
14. Liu, M.; Lu, Y.; Chen, W., PdAg nanorings supported on graphene nanosheets: highly methanol-tolerant cathode electrocatalyst for alkaline fuel cells. *Adv. Funct. Mater.* **2013**, *23*, 1289-1296.
15. Xu, H.; Yan, B.; Zhang, K.; Wang, J.; Li, S.; Wang, C.; Xiong, Z.; Shiraishi, Y.; Du, Y., Self-supported worm-like PdAg nanoflowers as efficient electrocatalysts towards ethylene glycol oxidation. *ChemElectroChem* **2017**, *4*, 2527-2534.
16. Ju, P.; Chen, J.; Chen, A.; Chen, L.; Yu, Y., N-Formylation of amines with CO<sub>2</sub> and H<sub>2</sub> using Pd–Au bimetallic catalysts supported on polyaniline-functionalized carbon nanotubes. *ACS Sustain. Chem. Eng.* **2017**, *5*, 2516-2528.
17. Li, T.; Huang, Y.; Ding, K.; Wu, P.; Abbas, S. C.; Ghausi, M. A.; Zhang, T.; Wang, Y., Newly designed PdRuBi/N-Graphene catalysts with synergistic effects for enhanced ethylene glycol electro-oxidation. *Electrochim. Acta* **2016**, *191*, 940-945.
18. Chen, D.; Sun, P.; Liu, H.; Yang, J., Bimetallic Cu–Pd alloy multipods and their highly electrocatalytic performance for formic acid oxidation and oxygen reduction. *J. Mater. Chem. A* **2017**, *5*, 4421-4429.
19. Chen, G.; Zhao, Y.; Fu, G.; Duchesne, P. N.; Gu, L.; Zheng, Y.; Weng, X.; Chen, M.; Zhang, P.; Pao, C. W.; Lee, J. F.; Zheng, N., Interfacial effects in iron-nickel hydroxide-platinum nanoparticles enhance catalytic oxidation. *Science* **2014**, *344*, 495-499.
20. Fu, G.; Liu, Z.; Chen, Y.; Lin, J.; Tang, Y.; Lu, T., Synthesis and electrocatalytic activity of Au@Pd core-shell nanothorns for the oxygen reduction reaction. *Nano Res.* **2014**, *7*, 1205-1214.
21. Kannan, R.; Kim, A. R.; Yoo, D. J., Enhanced electrooxidation of methanol, ethylene glycol, glycerol, and xylitol over a polypyrrole/manganese oxyhydroxide/palladium nanocomposite electrode. *J. Appl. Electrochem.* **2014**, *44*, 893-902.
22. Liu, D.; Xie, M.; Wang, C.; Liao, L.; Qiu, L.; Ma, J.; Huang, H.; Long, R.; Jiang, J.; Xiong, Y., Pd-Ag alloy hollow nanostructures with interatomic charge polarization for enhanced electrocatalytic formic acid oxidation. *Nano Res.* **2016**, *9*, 1590-1599.
23. Zhai, C.; Sun, M.; Zhu, M.; Song, S.; Jiang, S., A new method to synthesize sulfur-doped graphene as effective metal-free electrocatalyst for oxygen reduction reaction. *Appl. Surf. Sci.* **2017**, *407*, 503-508.
24. Wang, Y.; Shi, F.-F.; Yang, Y.-Y.; Cai, W.-B., Carbon supported Pd–Ni–P nanoalloy as an efficient catalyst for ethanol electro-oxidation in alkaline media. *J. Power Sources* **2013**, *243*, 369-373.
25. Wu, P.; Huang, Y.; Zhou, L.; Wang, Y.; Bu, Y.; Yao, J., Nitrogen-doped graphene supported highly dispersed palladium-lead nanoparticles for synergetic enhancement of ethanol electrooxidation in alkaline medium. *Electrochim. Acta* **2015**, *152*, 68-74.
26. Yu, X.; Pickup, P. G., Novel Pd–Pb/C bimetallic catalysts for direct formic acid fuel cells. *J. Power Sources* **2009**, *192*, 279-284.
27. Asset, T.; Serov, A.; Padilla, M.; Roy, A. J.; Matanovic, I.; Chatenet, M.; Maillard, F.; Atanassov, P., Design of Pd-Pb catalysts for glycerol and ethylene glycol electrooxidation in alkaline medium. *Electrocatal.* **2018**. doi.org/10.1007/s12678-017-0449-8.

- 1  
2  
3 28. Liu, Z.; Guo, B.; Tay, S. W.; Hong, L.; Zhang, X., Physical and electrochemical characterizations  
4 of PtPb/C catalyst prepared by pyrolysis of platinum(II) and lead(II) acetylacetonate. *J. Power Sources*  
5 **2008**, *184*, 16-22.
- 6 29. Shen, Y.; Gong, B.; Xiao, K.; Wang, L., In situ assembly of ultrathin PtRh nanowires to graphene  
7 nanosheets as highly efficient electrocatalysts for the oxidation of ethanol. *ACS Appl. Mater. Interfaces*  
8 **2017**, *9*, 3535-3543.
- 9 30. Xu, H.; Yan, B.; Zhang, K.; Wang, C.; Zhong, J.; Li, S.; Yang, P.; Du, Y., Facile synthesis of  
10 Pd-Ru-P ternary nanoparticle networks with enhanced electrocatalytic performance for methanol  
11 oxidation. *Int. J. Hydrogen Energy* **2017**, *42*, 11229-11238.
- 12 31. Ma, N.; Liu, X.; Yang, Z.; Tai, G.; Yin, Y.; Liu, S.; Li, H.; Guo, P.; Zhao, X. S., Carrageenan  
13 assisted synthesis of palladium nanoflowers and Their electrocatalytic activity toward ethanol. *ACS*  
14 *Sustain. Chem. Eng.* **2017**, *6*, 1133-1140.
- 15 32. Xu, H.; Yan, B.; Zhang, K.; Wang, J.; Li, S.; Wang, C.; Shiraishi, Y.; Du, Y.; Yang, P.,  
16 Ultrasonic-assisted synthesis of N-doped graphene-supported binary PdAu nanoflowers for enhanced  
17 electro-oxidation of ethylene glycol and glycerol. *Electrochim. Acta* **2017**, *245*, 227-236.
- 18 33. Lyu, L.-M.; Kao, Y.-C.; Cullen, D. A.; Sneed, B. T.; Chuang, Y.-C.; Kuo, C.-H., Spiny rhombic  
19 dodecahedral CuPt nanoframes with enhanced catalytic performance synthesized from Cu nanocube  
20 templates. *Chem. Mater.* **2017**, *29*, 5681-5692.
- 21 34. Ye, W.; Kou, S.; Guo, X.; Xie, F.; Sun, H.; Lu, H.; Yang, J., Controlled synthesis of bimetallic  
22 Pd-Rh nanoframes and nanoboxes with high catalytic performances. *Nanoscale* **2015**, *7*, 9558-9562.
- 23 35. Shen, M.; Huang, Y.; Wu, D.; Lü, J.; Cao, M.; Liu, M.; Yang, Y.; Li, H.; Guo, B.; Cao, R., Facile  
24 ultrafine copper seed-mediated approach for fabricating quasi-two-dimensional palladium-copper  
25 bimetallic trigonal hierarchical nanoframes. *Nano Res.* **2017**, *10*, 2810-2822.
- 26 36. Cheng, H.; Su, C.-Y.; Tan, Z.-Y.; Tai, S.-Z.; Liu, Z.-Q., Interacting ZnCo<sub>2</sub>O<sub>4</sub> and Au nanodots on  
27 carbon nanotubes as highly efficient water oxidation electrocatalyst. *J. Power Sources* **2017**, *357*, 1-8.
- 28 37. Zhou, L. N.; Zhang, X. T.; Wang, Z. H.; Guo, S.; Li, Y. J., Cubic superstructures composed of  
29 PtPd alloy nanocubes and their enhanced electrocatalysis for methanol oxidation. *Chem. Commun.*  
30 **2016**, *52*, 12737-12740.
- 31 38. Li, X.-X.; Chen, G.-F.; Xiao, K.; Li, N.; Ma, T.-Y.; Liu, Z.-Q.; Self-supported amorphous-edge nickel  
32 sulfide nanobrush for excellent energy storage. *Electrochim. Acta* **2017**, *255*, 153-159.
- 33 39. Sun, M.; Hu, J.; Zhai, C.; Zhu, M.; Pan, J., CuI as Hole-transport channel for enhancing  
34 photoelectrocatalytic activity by constructing CuI/BiOI heterojunction. *ACS Appl. Mater. Interfaces*  
35 **2017**, *9*, 13223-13230.
- 36 40. Xu, H.; Yan, B.; Li, S.; Wang, J.; Wang, C.; Guo, J.; Du, Y., N-doped graphene supported PtAu/Pt  
37 intermetallic core/dendritic shell nanocrystals for efficient electrocatalytic oxidation of formic acid.  
38 *Chem. Eng. J.* **2018**, *334*, 2638-2646.
- 39 41. Xu, H.; Yan, B.; Zhang, K.; Wang, J.; Li, S.; Wang, C.; Du, Y.; Yang, P., Sub-5nm monodispersed  
40 PdCu nanosphere with enhanced catalytic activity towards ethylene glycol electrooxidation.  
41 *Electrochim. Acta* **2018**, *261*, 521-529.
- 42 42. Ju, K.-J.; Liu, L.; Feng, J.-J.; Zhang, Q.-L.; Wei, J.; Wang, A.-J., Bio-directed one-pot synthesis of  
43 Pt-Pd alloyed nanoflowers supported on reduced graphene oxide with enhanced catalytic activity for  
44 ethylene glycol oxidation. *Electrochim. Acta* **2016**, *188*, 696-703.
- 45 43. Niu, W.; Gao, Y.; Zhang, W.; Yan, N.; Lu, X., Pd-Pb alloy nanocrystals with tailored composition  
46 for semihydrogenation: taking advantage of catalyst poisoning. *Angew. Chem.* **2015**, *54*, 8271-8274.
- 47  
48  
49  
50  
51  
52  
53  
54  
55  
56  
57  
58  
59  
60

- 1  
2  
3 44. Chen, X.; Wang, J.; Odoom-Wubah, T.; Jing, X.; Huang, J.; Li, Q.; Zheng, Y.,  
4 Microorganism-assisted synthesis of Au/Pd/Ag nanowires. *Mater. Lett.* **2016**, *165*, 29-32.
- 5 45. Yang, L.; Zhang, Z.; Nie, G.; Wang, C.; Lu, X., Fabrication of conducting polymer/noble metal  
6 composite nanorings and their enhanced catalytic properties. *J. Mater. Chem. A* **2015**, *3*, 83-86.
- 7 46. Peng, H. C.; Xie, S.; Park, J.; Xia, X.; Xia, Y., Quantitative analysis of the coverage density of Br<sup>-</sup>  
8 ions on Pd{100} facets and its role in controlling the shape of Pd nanocrystals. *J. Am. Chem. Soc.* **2013**,  
9 *135*, 3780-3783.
- 10 47. Xu, H.; Zhang, K.; Yan, B.; Wang, J.; Wang, C.; Li, S.; Gu, Z.; Du, Y.; Yang, P., Ultra-uniform  
11 PdBi nanodots with high activity towards formic acid oxidation. *J. Power Sources* **2017**, *356*, 27-35.
- 12 48. Xu, H.; Wang, J.; Yan, B.; Zhang, K.; Li, S.; Wang, C.; Shiraishi, Y.; Du, Y.; Yang, P., Hollow  
13 Au<sub>x</sub>Ag/Au core/shell nanospheres as efficient catalysts for electrooxidation of liquid fuels. *Nanoscale*  
14 **2017**, *9*, 12996-13003.
- 15 49. Yang, Y.; Wang, W.; Liu, Y.; Wang, F.; Zhang, Z.; Lei, Z., Carbon supported heterostructured  
16 Pd-Ag nanoparticle: Highly active electrocatalyst for ethylene glycol oxidation. *Int. J. Hydrogen*  
17 *Energy* **2015**, *40*, 2225-2230.
- 18 50. Jana, R.; Subbarao, U.; Peter, S. C., Ultrafast synthesis of flower-like ordered Pd<sub>3</sub>Pb nanocrystals  
19 with superior electrocatalytic activities towards oxidation of formic acid and ethanol. *J. Power Sources*  
20 **2016**, *301*, 160-169.
- 21 51. Feng, Y.; Bu, L.; Guo, S.; Guo, J.; Huang, X., 3D Platinum-lead nanowire networks as highly  
22 efficient ethylene glycol oxidation electrocatalysts. *Small* **2016**, *12*, 4464-4470.
- 23 52. Chen, S. S.; Yang, Z. Z.; Wang, A. J.; Fang, K. M.; Feng, J. J., Facile synthesis of bimetallic  
24 gold-palladium nanocrystals as effective and durable advanced catalysts for improved electrocatalytic  
25 performances of ethylene glycol and glycerol oxidation. *J. Colloid Interface Sci.* **2018**, *509*, 10-17.
- 26 53. An, L.; Chen, R., Recent progress in alkaline direct ethylene glycol fuel cells for sustainable  
27 energy production. *J. Power Sources* **2016**, *329*, 484-501.
- 28 54. Verduyck, J.; Van Hoof, M.; De Schouwer, F.; Wolberg, M.; Kurttepli, M.; Eloy, P.; Gaigneaux,  
29 E. M.; Bals, S.; Kirschhock, C. E. A.; De Vos, D. E., PdPb-catalyzed decarboxylation of proline to  
30 pyrrolidine: highly selective formation of a biobased amine in water. *ACS Catal.* **2016**, *6*, 7303-7310.
- 31 55. Li, S.-S.; Hu, Y.-Y.; Feng, J.-J.; Lv, Z.-Y.; Chen, J.-R.; Wang, A.-J., Rapid room-temperature  
32 synthesis of Pd nanodendrites on reduced graphene oxide for catalytic oxidation of ethylene glycol and  
33 glycerol. *Int. J. Hydrogen Energy* **2014**, *39*, 3730-3738.
- 34 56. Wei, R.-B.; Kuang, P.-Y.; Cheng, H.; Chen, Y.-B.; Long, J.-Y.; Zhang, M.-Y.; Liu, Z.-Q.,  
35 Plasmon-enhanced photoelectrochemical water splitting on gold nanoparticle decorated ZnO/CdS  
36 nanotube arrays. *ACS Sustainable Chem. Eng.* **2017**, *5*, 4249-4257.
- 37 57. Ali Shah, A.-u.-H.; Yasmeen, N.; Rahman, G.; Bilal, S., High electrocatalytic behaviour of Ni  
38 impregnated conducting polymer coated platinum and graphite electrodes for electrooxidation of  
39 methanol. *Electrochim. Acta* **2017**, *224*, 468-474.
- 40 58. Xu, H.; Wang, J.; Yan, B.; Li, S.; Wang, C.; Shiraishi, Y.; Yang, P.; Du, Y., Facile construction of  
41 fascinating trimetallic PdAuAg nanocages with exceptional ethylene glycol and glycerol oxidation  
42 activity. *Nanoscale* **2017**, *9*, 17004-17012.
- 43  
44  
45  
46  
47  
48  
49  
50  
51  
52  
53  
54  
55  
56  
57  
58  
59  
60

## For Table of Content Use Only

